Geometry, Energy, and Vibrational Frequencies of the Bis(dicyanomethylene)squarilium Dianion†

Bruno Lunelli,*,‡ Magda Monari, and Andrea Bottoni

Department of Chemistry "G.Ciamician", University of Bologna, 2 via F. Selmi, I-40126 Bologna, Italy

Received: September 29, 2000

Similarly to its 1,2-isomer, the bis(dicianomethylene)squaraine (BCSQ) atom connectivity can be a dianion, a radical anion, and a neutral, electron-poor species. This makes it attractive as a constituent unit of new materials. In the present paper we investigate the stable dianion, using theoretical calculation results to connect the geometry determined by X-ray diffraction of the single crystal of $Na_2BCSQ{\cdot}4H_2O$ and the vibrational frequencies determined by solution- and solid-state infrared and Raman spectroscopy of various neutral salts.

Introduction

Our long-lasting interest in cyclobutene derivatives[1] as chemical species,[2] which by themselves or as aggregates can give useful new chemical compounds or materials,[3] prompted us to investigate the relevant physicochemical properties of the title system, which is known as a dianion[4] ([3-(dicyanomethyl)-2,4-dioxocyclobutylidene]propanedinitrile ion(2−), CAS number 92-447-68-0; see Chart 1). Removal of one electron from the highest energy orbital might also yield a radical anion ($BCSQ^{\bullet-}$), and dismutation, or withdrawal of a second electron from the radical anion, should give a neutral (BCSQ), electron-poor species similar to the well-known electron acceptor tetracyanoquinodimethane (TCNQ). The easy synthesis[5] of the radical $BCSQ^{\bullet-}$ provided impetus to the investigation of $BCSQ^{2-}$.

To gain robust knowledge of the basic physicochemical properties of $BCSQ^{2-}$, that is geometry and vibrations, from measurements carried out necessarily in condensed phases by means of X-ray diffraction (XRD) and IR and Raman spectra, we planned to connect the new experimental information in such a way to build up a scaffolding of reciprocally reinforcing evidences. This required carrying out theoretical computations of such quantities for the free dianion.

Hereafter we report, compare, and discuss the outcomes of the calculations and the measurements.

Experimental Section

$BCSQ^{2-}$ Salts. The disodium salt was synthesized following a reported procedure.[3] The potassium, rubidium, and cesium salts were obtained as anhydrous, crystalline precipitates by mixing concentrated water solutions of stoichiometric quantities of the sodium salt and potassium nitrate and rubidium or cesium chloride. The thallium salt, prepared by mixing a hot solution of the sodium salt with an excess of thallium acetate, was a powder without evidence of becoming crystalline even after keeping it 4 h at 100 °C in the mother solution ("Ostwald ripening"). These salts, as well as the anhydrous, hygroscopic sodium salt, have an orange-red color, in contrast to the yellow color of the hydrated salt $Na_2BCSQ{\cdot}4H_2O$, which crystallizes from the hot saturated water solution. The cesium and thallium salts are very slightly soluble in acetonitrile, much more in dimethyl sulfoxide (DMSO): about 17 and 37 mg in 100 μL at 25 °C, respectively. The deuterated hydrate $Na_2BCSQ{\cdot}4D_2O$ was prepared from the stoichiometric quantities of Na_2BCSQ and D_2O in an Ar atmosphere.

CHART 1

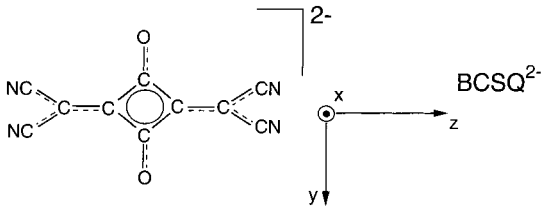

Single crystals of yellow $Na_2BCSQ{\cdot}4H_2O$ were grown by slow cooling of the warm (about 40 °C) water solution. Their composition was established by thermal analysis, and confirmed by the results of XRD. By evaporation of its aqueous solution, also the cesium salt gave needlelike crystals, but too small to obtain satisfactory results from the presently available apparatus. We are trying to obtain Tl_2BCSQ crystals from DMSO solutions.

Thermogravimetry (TG) utilized a Mettler TG 50 thermobalance, as a part of a Mettler TA3000 system; the sample was heated at a rate of 2 K min^{-1} from 30 to 220 °C in a controlled air stream at atmospheric pressure. The weight change corresponds to the loss of four molecules of water per mole of Na_2BCSQ, from which the above formula was derived. The anhydrous salts did not change weight.

Differential scanning calorimetry (DSC) exploited a Mettler DSC 20 accessory; the sample was heated at a rate of 2 K min^{-1} from 30 to 250 °C. The anhydrous salts did not show peaks. The sample of $Na_2BCSQ{\cdot}4H_2O$ was put into a flat, punctured aluminum box; the TG curve, its first derivative, and the DSC curve indicate that substantial water loss starts at 55 °C and ends at 105 °C. There is no evidence of other hydrates. The area under the single peak[6] corresponds to 248 kJ per formula weight, an approximate value for $\Delta H°_{373\ K}$ of the process $Na_2BCSQ{\cdot}4H_2O(s) \rightarrow Na_2BCSQ(s) + 4H_2O(g)$. The difference, about 85 kJ, with 4×40.65 kJ $\approx$ 163 kJ, which refers to the

† Part of the special issue "Aron Kuppermann Festschrift".

* To whom correspondence should be addressed. E-mail: blunelli@ciam.unibo.it.

‡ Also at the Istituto di Spettroscopia Molecolare CNR, via Gobetti 101, I-40129 Bologna, Italy.

10.1021/jp003580v CCC: $20.00
Published on Web 02/17/2001

TABLE 1: Crystal Data and Experimental Details for $Na_2BCSQ{\cdot}4H_2O$

empirical formula	$Na_2C_{10}N_4O_2{\cdot}4H_2O$	D_c, Mg m^{-3}	1.547
M	326.18	μ(Mo Kα), mm^{-1}	0.179
temp, K	293(2)	F(000)	664
wavelength, Å	0.710 69	cryst size, mm	0.075 × 0.10 × 0.30
cryst sym	monoclinic	θ limits, deg	2−25
space group	$C2/c$ (no. 15)	scan mode	ω
a, Å	10.829(2)	no. of reflns collected	2541 ($\pm h$, $+k$, $\pm l$)
b, Å	20.295(2)	no. of unique obsd reflns [$F_o > 4\sigma(F_o)$]	1220
c, Å	6.701(3)	goodness of fit on F^2	0.979
β, deg	108.02(2)	R_1 (F),[a] wR_2 (F^2)[b]	0.0318, 0.0690
cell vol, Å^3	1400.5(7)	weighting scheme a, b	0.0396, 0.000
Z	4	largest diff peak and hole, e·Å^{-3}	0.23 and −0.17

[a] $R_1 = \sum||F_o| - |F_c|/\sum|F_o||$. [b] $wR_2 = [\sum w(F_o^2 - F_c^2)^2/\sum w(F_o^2)^2]^{1/2}$, $w = 1/[\sigma^2(F_o^2) + (aP)^2 + bP]$, $P = (F_o^2 + 2F_c^2)/3$.

TABLE 2: Selected Bond Lengths (Å), Contacts (Å), and Angles (deg) in $Na_2BCSQ{\cdot}4H_2O$

C(1)−C(3)	1.465(3)	C(4)−C(5)	1.419(3)
C(2)−C(3)	1.449(3)	C(5)−N(1)	1.143(3)
C(1)−O(1)	1.232(3)	C(4)−C(6)	1.422(3)
C(2)−O(2)	1.256(3)	C(6)−N(2)	1.139(3)
C(3)−C(4)	1.381(3)	O(2)···O(1w^{III})[a,b]	2.933(2)
O(1)···O(1w)[a]	2.801(3)	O(2)···O(2w^{IV})[a,b]	2.907(3)
Na(1)···O(1w)[a]	2.411(2)	Na(2)···O(2w^{XVII})[a,b]	2.365(2)
Na(1)···O(2w^{IX})[a,b]	2.438(2)	Na(2)···N(2^{XI})[b]	2.433(2)
Na(1)···N(1^{XI})[b]	2.473(2)	Na(2)···N(1^{VII})[b]	2.717(2)
Na(1)···Na(2^{XV})[b]	3.680(2)		
C(3)−C(2)−C(3^{I})[b]	91.6(2)	C(3)−C(4)−C(6)	122.0(2)
C(2)−C(3)−C(1)	89.0(2)	C(6)−C(4)−C(5)	117.2(2)
C(3)−C(2)−O(2)	134.2(1)	C(4)−C(5)−N(1)	178.8(2)
C(3)−C(1)−O(1)	134.8(1)	C(4)−C(6)−N(2)	179.1(2)
C(3)−C(4)−C(5)	120.7(2)	C(4)−C(3)−C(2)	134.7(2)
C(4)−C(3)−C(1)	136.3(2)	O(1w)−H(1B)···O(2^{III})[a,b]	147(3)
O(1w)−H(1A)···O(1)[a]	157(3)	O(2w)−H(2A)···O(2^{IV})[a,b]	152(2)
O(2w)−H(2B)···O(1w^{XIX})[a,b]	170(3)		

[a] The two water oxygens in the asymmetric unit are labeled O(1w) and O(2w), respectively, to distinguish them from the dianion oxygens. [b] Symmetry codes: I, $-x$, y, $-z + 0.5$; III, $-x$, $-y + 1$, $-z$; IV, $-x + 1$, $-y + 1$, $-z + 1$; VIII, $-x - 0.5$, $-y + 0.5$, $-z$; IX, $x - 1$, y, $z - 1$; XI, $-x - 0.5$, $y - 0.5$, $-z + 0.5$; XV, $-x$, $-y$, $-z + 1$; XVII, $x - 1$, $-y$, $z - 0.5$; XIX, $x + 0.5$, $-y + 0.5$, $z + 0.5$.

vaporization of 4 mol of water at 100 °C, is a measure of the energy required to convert the hydration water into the pure liquid.

The equilibrium water pressure over the $Na_2BCSQ{\cdot}4H_2O$(s)−Na_2BCSQ(s)−H_2O(g) system was measured at the laboratory temperature of 23 °C utilizing a previously described apparatus,[7] but using a Baratron with an end scale of 100 Torr. We found 2 Torr = 267 Pa ± 20% as the equilibrium value, considerably lower than the 2810 Pa of pure water at this temperature. This result agrees with the considerable energy required to remove the water from the hydrate, and the strong bonding of the H_2O molecules in the $Na_2BCSQ{\bullet}4H_2O$ evidenced by XRD.

XRD from a Single Crystal of $Na_2BCSQ{\cdot}4H_2O$. A yellow crystal of the title compound was sealed inside a thin-walled glass capillary. The diffraction experiments were carried out at room temperature on a fully automated CAD4 diffractometer. The unit cell parameters were determined from 25 randomly selected reflections by using automatic search, indexing, and least-squares routines. A summary of the experimental procedures and data collection is given in Table 1. Intensity data were corrected for Lorentz and polarization effects. An empirical absorption correction was applied by using the azimuthal scan method.[8] The structure was determined by direct methods in the centric space group $C2/c$ using SHELXS 86[9] and successfully refined by full-matrix least-squares calculations. The hydrogen atoms in H_2O were located in a Fourier difference map. The final refinement on F^2 proceeded by least-squares calculations (SHELXL 93[10]) using anisotropic thermal parameters for all the non-hydrogen atoms and fixed isotropic parameters for the hydrogen atoms 1.2 times the value of the average isotropic thermal factor of the oxygen atom.

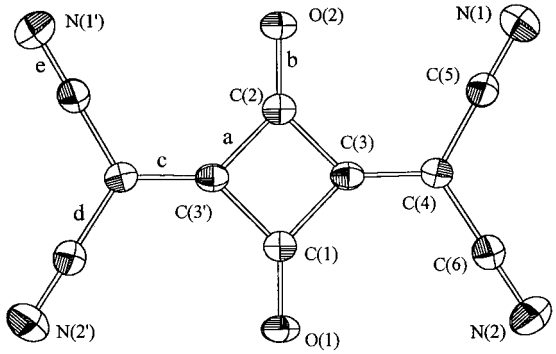

Figure 1. Geometry of $BCSQ^{2-}$ in the crystal of $Na_2BCSQ{\cdot}4H_2O$. Only the C_2 axis through the two carbonyls of the D_{2h} free dianion is retained in the crystal. Thermal ellipsoids are drawn at a probability of 50%.

Selected interatomic distances and angles are reported in Table 2, while a representation of the dianion with the symbols used in Table 2 is given in Figure 1.

UV−Vis−Near-IR Spectrum. The absorbance spectra of Cs_2BCSQ were measured in its DMSO solutions (8.7×10^{-4} and 7.9×10^{-5} m) in 2 mm thick quartz cells by using a Cary 5 spectrophotometer, from 200 to 2500 nm. The results are shown in Figure 2 for the region 200−800 nm; there are no detectable features from 800 to 2500 nm (4000 cm^{-1}), where the measurement of the IR spectra starts.

IR Spectra. The FT-IR spectra of Na_2BCSQ, $Na_2BCSQ{\cdot}4H_2O$, $Na_2BCSQ{\cdot}4D_2O$, Tl_2BCSQ, and Cs_2BCSQ were recorded

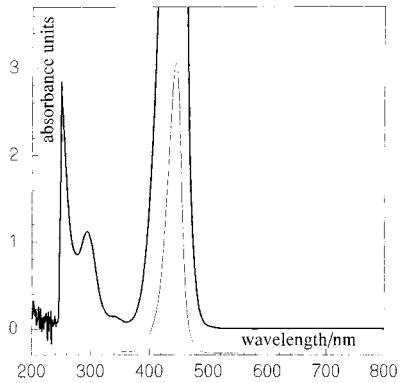

Figure 2. Vis−UV spectrum of Cs_2BCSQ as a solution in DMSO.

at about 25 °C from 4000 to 40 cm^{-1} using a Bruker IFS 113v, operating in a "vacuum", that is, at about 15 Torr of 99% N_2 [detector DTGS, apodization function three-term Blackman-Harris, resolution 1 cm^{-1}, beam splitters Ge on KBr (4000−400 cm^{-1}) and Mylar 3.5 μm (700−125 cm^{-1}), 6 μm (480−80 cm^{-1}), and 12 μm (220−40 cm^{-1})]. Two different sample forms were used: paraffin oil and hexachlorobutadiene mull for all the compounds and solutions [25 μm thick solutions of 10 and 2 mg of the cesium salt in 100 μL of DMSO and fully deuterated DMSO (DDMSO); 12 μm thick solutions of 37 and 8 mg in 100 μL of DMSO for the thallium salt]. DMSO dissolves KRS5, so except for saturated Tl_2BCSQ it was necessary to use ZnSe, Si, or ultrahigh molecular weight polyethylene (UHMWPE) windows. The mulls of the hydrated species were squeezed between ZnSe (region 3945−500 cm^{-1}), UHMWPE (spectral region 700−40 cm^{-1}), or Si windows contained in a vacuum-tight cell for liquids[11] to avoid loss of water.

In view of the possibility that the solute−solvent interactions modify the spectrum of the solvent,[12] we also measured the spectrum of solutions of CsI in DMSO of the same molality as those of Cs_2BCSQ, but in the region 4000−500 cm^{-1} we found only negligible differences with that of pure DMSO.

The same applies to the Tl_2BCSQ solutions, except for the DMSO bands at 335 and 383 cm^{-1}, whose intensity appears higher in solution than in the pure solvent. These features were attributed to two deformations of the >S═O group,[13] whose polarity plausibly increases for the molecules interacting with the cations.

The spectrum of the paraffin oil mull of Cs_2BCSQ (with the absorbance of the oil subtracted) from 2500 to 400 cm^{-1} was attached to that from 402 to 80 cm^{-1} by software, adjusting the intensity of the latter spectra so that the band at 417 cm^{-1} had the same intensity as in the former. The combined spectrum is shown in Figure 3. The frequencies and intensities of the main bands observed in the mentioned substances are listed in Table 3.

Raman Spectra. The Raman spectrum of Cs_2BCSQ powder was measured by means of a Bruker RFS (Raman Fourier spectrometer) 100 with a liquid nitrogen cooled Ge detector at a resolution of 4 cm^{-1} in the backscattering 180° geometry using as exciting radiation the 1064 nm line of a focused continuous wave (cw) Nd^{3+}:YAG. As usual,[14] the bands stay sharp even in the solid.

Initially we tried to measure the polarized Raman spectrum of a 0.57 *m* solution of Na_2BCSQ in DMSO by using a Renishaw 1000, a dispersive charge-coupled-device (CCD) detector Raman spectrometer, with the He−Ne 632.8 line as the lowest frequency exciting radiation, but fluorescence was so strong to allow observation of only a few bands. The spectrum shown in Figure 4 was measured in the backscattering mode by means of the Bruker RFS 100 using focused 1064 nm radiation at a resolution of 1 cm^{-1}. The frequencies and intensities of the main bands observed in the mentioned substances are listed in Table 3.

Computational Methods. The computations were carried out at the DFT level,[15] using the Gaussian 98[16] series of programs. The 6-31G* and 6-311G** basis sets[17] were employed.

The geometry of $BCSQ^{2-}$ was fully optimized by means of the gradient method available in Gaussian 98. The computed values of the geometrical parameters are collected in Table 4, where the symbols for angles and distances are those of Figure 1. The computed harmonic vibrational frequencies and IR and Raman intensities are listed in Table 5. A single scaling factor of 0.96 and 0.99 has been used for B3LYP and BLYP, respectively.[18]

Results and Discussion

1. Crystal Packing and Molecular Geometry of $Na_2BCSQ\cdot 4H_2O$. The crystal is built up of discrete dianions, sodium cations, and water molecules (four per formula unit) held together by a tridimensional array of cation−anion and cation−water interactions and hydrogen bridges. Both anions and cations are located on 2-fold symmetry axes, and the independent part of the cell consists of half an anion, two half-cations and two water molecules. The packing (Figure 5) can be described in terms of layers, nearly perpendicular to the *c* axis, that contain cations and planar dianions. The sodium cations exhibit octahedral coordination polyhedra sharing two edges, so that columns of connected octahedra run across the layers. The coordination polyhedra are not chemically equivalent because Na(1) is surrounded by four water oxygens and two nitrogens while Na(2) is bound to two water oxygens and four nitrogens. It should be noted that the oxygen atoms in the anions are not coordinated. Although the four CN groups are equivalent under the D_{2h} symmetry of the isolated anion, the vicinal groups are not equivalent in the crystal. N(2) is coordinated only to Na(2) [2.433(2) Å], and N(1) is coordinated to both cations [N(1)−Na(1) 2.473(2) Å, N(1)−Na(2) 2.717(2) Å]. The water molecules play an important role in the crystal architecture. They are coordinated to the sodium cations [Na−OH_2 distances in

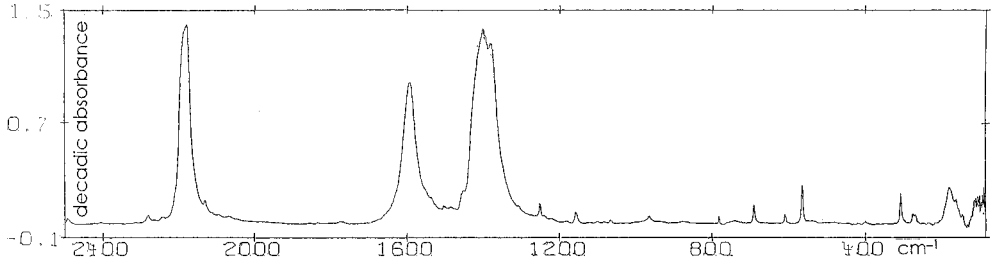

Figure 3. IR absorbance spectrum of Cs_2BCSQ as a paraffin oil mull (oil spectrum subtracted).

TABLE 3: Experimental Infrared (IR) and Raman (R) Data at Maximum of Bands for the Cesium, Thallium (I), and Sodium Neutral, Anhydrous and Hydrated Salts of the $BCSQ^{2-}$ Dianion

IR														R			
Cs_2BCSQ				Tl_2BCSQ				Na_2BCSQ		$Na_2BCSQ\cdot 4H_2O$		$Na_2BCSQ\cdot 4D_2O$		Na_2BCSQ		Cs_2BCSQ	
in DMSO		mull		in DMSO		mull		mull		mull		mull		in DMSO		powder	
freq/ cm^{-1}	rel intens[a]	freq/ cm^{-1}	rel intens[a]	freq/ cm^{-1}	rel intens[a]	freq/ cm^{-1}	rel intens[a]	freq/ cm^{-1}	rel intens[a]	freq/ cm^{-1}	rel intens[a]	freq/ cm^{-1}	rel intens[a]	freq/ cm^{-1}	rel intens[b]	freq/ cm^{-1}	rel intens[a]
		57	16					71	1	62	35	61	16			56	2
		80	18											76	34	83	49
90	4	90	20							95	30	93	13	114	26		
		110	18							111	33			138	32p	150	27
125	4	127	6			130	75	117	23	124	51	122	37			178	9
		139	9											225	13	230	18
		159	16			162	80	155	27	158	51	157	35	390	52p	401	35
174	3	175	21	174	5	194	89	208	70b	191	50	189	36	465	8	470	2
										218	48	213	38	497	6	490	2
258	1	267	6	258	2	263	6			250	20			616	9p	613	7
		273	7			274	7	278	24	270	12	267	12	slv		675	9
310	2	305	16	310	5	318	20	316	20			316	sh	781	8p	783	
												386	30b	991	6p	974	2
										470	50b	467	30b	1023	14p	1026	2
568	4	566	19	568	8	566	42	565	45			570	58				
611	<1	611	9	610	3	610	20	613	28	621	16	621	7	1102	16	1124	16
616	1			616	3											1228	2
685	2	693	10	686	2	692	29	699	26	702	12	702	25	1229	11	1246	7
		723	2	708	3	723	17	722	19	722	11			1382	12p		
		740	2	738		739	15							1382	12p		
792	1	782	4	782	1	782	20	781	6	781	12	781	22	1459	8		
								855	4	855	9			1545	17p	1543	9
953	2	966	5	957	14	965	9			955		955	6	1750	5p	1765	1
										979		967	3	2166	44	2172	100
slv		1067	2	slv		1067	32							2201	100p	2207	98
1150	2	1158	7	1155	2	1157	35	1166	18	1150	10	1150	5				
		1181	2							1178	30	1180	20				
												1223[d]	48				
1237	2	1251	12	1240	4	1251	48	1254	29	1249	40	1250	39				
				1293	3	1307											
				1314	3												
						1366	90										
1383	100	1377	95	1376	98	1376	100	1376	87	1376	79						
		1401	97														
		1456	40			1457	94	1455	100	1453	100	1445	99				
												1462	87				
		1544		1533	19	1536	10	1522	sh	1532	46	1536	75				
1590	57	1593	71	1589	100	1610	35	1596	41	1582	49	1590	98				
						1620	37										
										1654		1648	16				
										1669[c]	44						
				2170	sh					2185	56	2185	92				
2167	20	2178	100	2168	66	2179	54	2190	58	2195	61	2196	99				
2180	66	2185	98	2181	62	2194	sh	2223	sh	2208	59	2211	100				
												2284	11				
												2427	33				
												2487[d]	60				
												2522[d]	53				
												2597[d]	65				
												2615[d]	62				
										3390[c]	43b						
										3512[c]	50b						

[a] Rounded to the next integer. Intensities lower than 1 are not reported. [b] Referred to parallel polarization. [c] Feature attributed to the presence of H_2O. [d] Feature attributed to the presence of D_2O. p means polarized, b broad, sh shoulder, and slv the region obscured by a strong solvent band.

the range 2.365−2.438(2) Å] and further stabilize the crystal by establishing a network of strong hydrogen bonds. Half the water molecules [O(1w)] participate in two hydrogen bonds, connecting the oxygens of the dianions in adjacent sheets [H(1A)···O(1) 2.06 Å, H(1B)···O(2) 2.26(2) Å]; the second half [O(2w)] participate in one hydrogen bond which connects one oxygen of the dianion [H(2A)···O(2) 2.20(2) Å]. The remaining hydrogen connects the two sets of inequivalent water molecules to each other [H(2B)···O(1w) 2.07(2) Å], and therefore all the water hydrogen-bonding potentiality is exploited. Each dianion in the assembly makes six hydrogen bonds through the two oxygen atoms, four at O(2) and two at O(1).

The geometry of the anion is shown in Figure 1; it is strictly planar (the deviations from the average plane do not exceed ±0.05 Å), and the carbonyl groups are placed along a crystallographic 2-fold symmetry axis. The imposed symmetry is therefore only C_2, but due to the planarity, it is C_{2v} within experimental errors and would be D_{2h} if nitrogen and oxygen atoms were not involved in quite different bonding interactions. Some deviations from the highest symmetry exhibited by the anion are worth discussing because they allow insights into its electronic structure. It should be noted that the different crystal force fields experienced by the carbonyl oxygens in the anion produce measurable effects on the carbon−oxygen distances

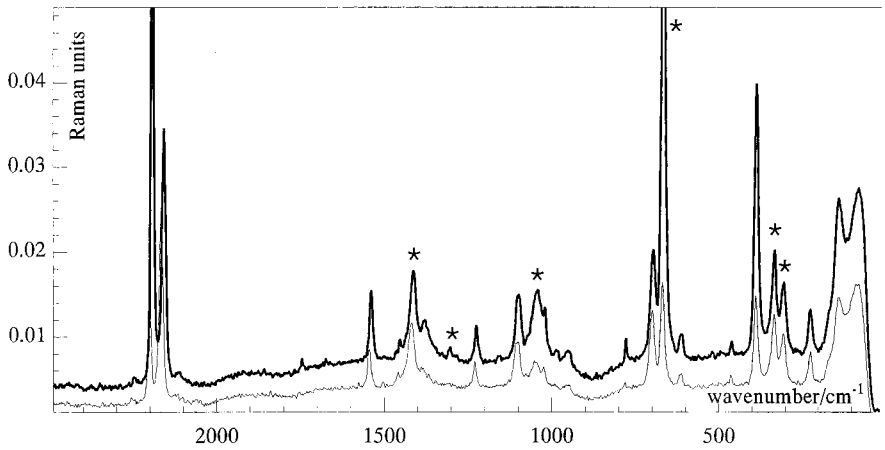

Figure 4. Polarized Raman spectrum of a Na_2BCSQ solution in DMSO. Asterisks indicate solvent bands.

TABLE 4: Geometrical Parameters Computed for $BCSQ^{2-}$ and Average Values Observed in the $Na_2BCSQ{\cdot}4H_2O$ Crystal

		computed values[a]			
		B3LYP		BLYP	
symbol from Figure 5	av exptl value[a,b]	6-31G*	6-311G**	6-31G*	6-311G**
a	1.457	1.475	1.475	1.490	1.489
b	1.244	1.235	1.230	1.247	1.241
c	1.381	1.407	1.404	1.419	1.416
d	1.421	1.422	1.419	1.429	1.426
e	1.141	1.172	1.164	1.185	1.177
∠*ab*	134.5	135.4	135.3	135.4	135.3
∠*ac*	135.5	134.6	134.7	134.6	134.7
∠*cd*	121.3	122.6	122.6	122.6	122.6
∠*de*	179.0	176.6	176.6	176.7	176.7

[a] Bond distances are in angstroms and angles in degrees. [b] Average over the values determined in the $Na_2BCSQ{\cdot}4H_2O$ crystal.

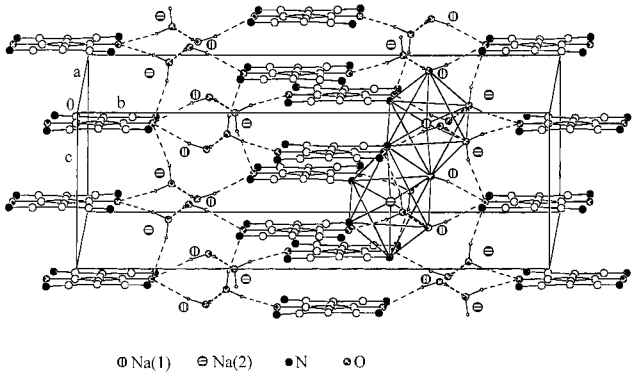

Figure 5. Crystal packing of $Na_2BCSQ{\cdot}4H_2O$, evidencing the layers containing anions and cations and the coordination polyhedra around the sodium ions. Dashed lines indicate the hydrogen bonds.

CHART 2

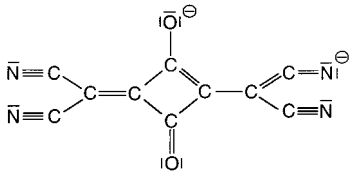

[C(1)−O(1) 1.232 Å, C(2)−O(2) 1.256(3) Å], the longer distance being that of the oxygen involved in four hydrogen bonds.

The C−C bond distances show that the four-membered ring is nearly regular and with significant double bond character [C(1)−C(3) 1.465(3) Å, C(2)−C(3) 1.449(3) Å, average 1.457 Å]. The C(ring)−C(CN) distance [1.381(3) Å] is almost pure double bond. The slight difference in the C(ring)−C(ring) distances, on the other hand, is significant in terms of estimated standard deviations and can be related to the previously analyzed asymmetries observed in the C−O distances. Also the distances in the C−C≡N groups show a tendency toward asymmetry [C(4)−C(5)−N(1) 1.419(3) and 1.143(3) Å, C(4)−C(6)−N(2) 1.422(3) and 1.139(3) Å]. These deviations from the idealized D_{2h} symmetry are truly small but significantly concerted and can be attributed to unbalanced charge accumulation on O(2), N(1), and N(1′) with respect to O(1), N(2), and N(2′), as a consequence of the nonequivalence of their polar interactions discussed above.

In conclusion the gross distribution of long and short distances in the dianion primarily conforms to the π electronic structure depicted by the electronic formula of Chart 1. The minor bond perturbations give evidence that canonical formulas which localize the negative charge on the most electronegative atoms (see Chart 2) play a non-negligible role. The asymmetric bond interactions in the crystal determine an increased contribution of this structure (and the equivalent formulas under the crystallographically imposed C_2 symmetry), which is responsible for the observed geometric effect.

In the dianion CDCB (1,2-carbodicyanocyclobutene-3,4-dione[1]), which can be considered the 1,2-analogue of the present 1,3-dianion, the bond length distributions are obviously different. In the former the C(ring)−C(ring) distance between the carbons bearing the $C(CN)_2$ groups is the shortest one [1.422(6) Å] and the C(O)−C(O) separation the longest one [1.475(6) Å]. The two remaining bonds in the ring are 1.456 and 1.472(6) Å, and the overall mean value is 1.458 Å, almost equal to that in the present dianion. On the other hand, the C(ring)−$C(CN)_2$ interaction [1.380(3) Å] has a significant double bond character as observed in the trans dianion (see above) and in the tetrasubstituted derivative of the squarate ion $[C_4\{C(CN)_2\}_4]^{2-}$ [1.394 and 1.381(4) Å].[4]

2. Computational Results. To compute the harmonic force field for $BCSQ^{2-}$, we choose a density functional theory (DFT) approach.[15] DFT-based methods have become more and more popular, during the past decade, as an alternative to traditional correlated ab initio methods based on Moller−Plesset theory (MP2, MP3, or higher) or configuration interaction (CI). This popularity stems in large measure from the computational expedience of the DFT methods (which provide the possibility of including electron correlation in the computations of large chemical systems), and the discovery of new and more accurate exchange-correlation energy functionals. Recent evidence has

TABLE 5: Fundamental Vibrational Frequencies Calculated for the $BCSQ^{2-}$ Free Dianion and Proposed Assignment of Observed Bands

		calculated by								assigned to			
		B3LYP[a]				BLYP[b]				feature observed in			
		6-311G**		6-31G*		6-311G**		6-31G*		IR		Raman	
vib no.	sym spec	freq/ cm^{-1}	IR/R intens[c]	freq/ cm^{-1}	IR/R intens[c]	freq/ cm^{-1}	IR/R intens[c]	freq/ cm^{-1}	IR/R intens[c]	freq/ cm^{-1}	rel intens	freq/ cm^{-1}	rel intens
1	b_{3u}	41	2	41	2	42	3	43	3	n.o.			
2	a_u	43		44		43		44					
3	b_{1g}	60	<1	61	<1	58	<1	59	<1				
4	b_{2u}	65	1	64	1	64	1	62	1	90	4		
5	b_{3g}	118	5	115	5	118	5	113	4			114	26
6	a_g	127	38	125	41	126	38	125	41			138	32p
7	b_{1u}	150	12	148	13	148	10	147	12	125	4		
8	b_{3u}	163	25	162	30	163	22	163	27	174	3		
9	b_{2g}	173	<1	172	<1	174	<1	173	<1				
10	b_{3g}	216	23	213	23	211	24	208	23			225	13
11	b_{2u}	254	1	253	1	248	1	247	1				
12	b_{3u}	267	2	265	2	265	3	263	3	258	1		
13	b_{1u}	286	3	281	3	277	2	273	3	310	2		
14	a_g	368	49	368	46	363	51	362	47			390	52p
15	b_{3g}	473	10	466	11	464	14	457	15			465	8
16	b_{1g}	489	7	487	8	479	5	475	6			447	6
17	b_{2g}	492	6	487	9	480	5	477	6			497	6
18	b_{2u}	493	2	487	2	486	2	479	2				
19	a_u	505		499		494		479					
20	b_{3u}	611	35	605	45	602	25	594	32	568	4		
21	a_g	628	2	623	2	621	1	615	<1			616	7p
22	b_{1u}	628	13	623	15	621	9	615	10	610	1		
23	b_{2g}	643	4	639	6	636	3	627	4				
24	a_g	648	18	646	18	640	18	638	18			675	9
25	b_{1g}	661	<1	640	<1	640	<1	628	<1				
26	b_{1u}	673	41	674	32	666	39	667	32	685	2		
27	b_{3u}	792	1	699	<1	781	1	698	<1	792	1		
28	b_{3g}	794	1	788	1	781	5	775	2				
29	a_g	1006	8	1007	6	992	2	994	2			1023	14p
30	b_{2u}	1034	13	1077	13	1010	11	1016	10	1067	1		
31	b_{3g}	1051	131	1061	127	993	79	1004	74				
32	b_{1u}	1114	74	1121	66	1086	48	1095	42	1150	2		
33	b_{3g}	1194	42	1199	42	1171	44	1177	42			1229	11
34	b_{2u}	1206	8	1213	7	1187	6	1192	6	1237	2		
35	b_{1u}	1348	2419	1363	2383	1332	1603	1345	1558	1383	100		
36	a_g	1506	8	1516	7	1475	1	1484	1			1545	17p
37	b_{2u}	1621	1038	1647	957	1593	851	1621	773	1590	57		
38	a_g	1744	35	1765	26	1705	15	1726	11			1750	5p
39	b_{3g}	2166	1433	2176	1387	2120	1391	2128	1318			2166	44
40	b_{2u}	2166	539	2177	537	2122	486	2129	480	2179	64		
41	b_{1u}	2189	1220	2199	1205	2146	1068	2154	1048	2194	sh		
42	a_g	2206	1165	2216	1065	2161	1269	2170	1149			2201	100p

[a] Scaled by 0.932 (0.965 for frequencies) as one-scale factor. [b] Scaled by 0.98 (0.99 for frequencies); see the Experimental Section. [c] IR intensity/(km mol^{-1}), R intensity/($Å^4$ amu^{-1}), rounded to the next integer; sh means observed as shoulder and n.o. not observed.

shown that these new functionals are capable of producing not only correct energetics and geometries for organic molecules, but also accurate molecular force fields and vibrational frequencies. In particular Handy and co-workers,[19] Pople and co-workers,[20] and Raghavahari et al.[21] showed that functionals including nonlocal corrections provide significantly better results than the Hartree−Fock method with similar computational effort. They also appear to be more reliable than correlated MP2 methods, which, for instance, do not properly describe certain vibrations of multiple bonds and some asymmetric vibrations, such as the one in ozone. Another important feature of the DFT approach is represented by a faster convergence with respect to an improvement of the basis set quality than that observed in conventional correlated methods. This is due to the fact that the role of the basis functions is only that of properly describing the occupied molecular orbitals and not the empty correlating orbitals. Thus, smaller basis sets are in general required in DFT.

In the present paper we used two different nonlocal functionals that are usually considered as the most promising ones in the computations of harmonic force fields: the pure BLYP functional,[22] which contains the Becke corrections, and the hybrid Becke three-parameter exchange B3LYP[23] functional. The computations employed the two 6-31G* and 6-311G** basis sets,[16] which represent a good compromise between accuracy and computational expedience. The harmonic vibrational frequencies and spectroscopic intensities were computed on the fully optimized geometries of $BCSQ^{2-}$ by means of the gradient method available in Gaussian 98. A single scaling factor (different for B3LYP and BLYP, as reported in the Computational Methods) for the frequencies was used,[17] because the initial stage of the assignment, the neglect of anharmonicities, and the exclusive condensed-state origin of the experimental frequencies did not seem to be consistent with the use of multiscale factors.

At all computational levels the system was found to be planar and characterized by a D_{2h} symmetry. Inspection of Table 4 shows the following.

(i) The two functionals provide very similar geometries. Only some lengthening of the various bonds is observed on passing from the hybrid B3LYP to the pure BLYP: for instance, with the 6-31G* basis, the C−C bond of the four-membered cycle (parameter *a*) varies from 1.465 to 1.490 Å, while the C═O

(*b*) and C≡N (*e*) bond distances vary from 1.235 and 1.172 to 1.247 and 1.185 Å, respectively.

(ii) The geometries obtained with the two basis sets are almost identical. The only change on passing from the 6-31G* level to the 6-311G** level is a slight shortening of the various bond lengths: the most significant, even if very small, is observed in the C≡N bond, which is 1.172 Å at the B3LYP/6-31G* level and becomes 1.164 Å at the B3LYP/6-311G** level.

(iii) A comparison between the computed values and the average experimental values, also reported in Table 4, shows that the DFT (mainly the BLYP functional) overestimates the C(1)−C(3) (*a*), C(3)−C(4) (*c*), and C(5)−N(1) (*e*) bond lengths while C(1)−O(1) (*b*) and C(4)−C(5) (*d*) are satisfactorily predicted. Parameters *a*, *c*, and *e* are calculated to be about 0.02 and 0.04 Å too long at the B3LYP and BLYP levels, respectively, while *b* (experimental value 1.244 Å) ranges between 1.230 (B3LYP/6-311G**) and 1.247 (BLYP/6-31G*) Å, and *d* (experimental value 1.421 Å) is in the range 1.419−1.429 Å.

3. Vibrational Frequencies of $BCSQ^{2-}$. As detailed in the previous section, in the present investigation of the dianion, we computed frequencies and intensities for the isolated dianion in the double harmonic (mechanic and electric) approximation. The absence of hydrogen nuclei removes the main source of anharmonicity, but the extended conjugation, the relatively large amplitude calculated for some nuclear displacements, and the overestimation of some internuclear distances (see the Computational Results) makes us prepared to see appreciable differences between calculated and observed IR intensities and frequencies.

3.a. Data Selection. Since the theoretical frequencies and intensities concern the isolated dianion $BCSQ^{2-}$, before comparing them with the spectroscopic data, we must show how suitable the latter are to such a purpose. To comply with this condition, the sample should consist of an ensemble where the dianion is in a situation as near as possible to the free state. Since our samples are necessarily macroscopic,[24] we must accept at least the perturbations due to the presence of many other anions and of the number of cations sufficient to obtain electrical neutrality. No known $BCSQ^{2-}$ salt has appreciable vapor pressure; thus, such perturbations could be minimized by choosing a bulky and univalent cation,[25] and examining the salt in solution. There, due to the interaction of the dianion also with the solvent molecules, the long-range interactions with the other ions are less strong and regular than in a crystal. Ion pairing[26] may occur, but cations of the type indicated should keep this possibility to a minimum. These considerations indicate that the best sample is a solution of the cesium (followed by monovalent thallium) salt, because the even bulkier tetraalkylammonium cations would add their own, untagged and superposing absorptions. The only good solvent we found was the basic, aprotic DMSO, which preferentially solvates the cations. However, it is known that solution spectra may include features attributable to the ensemble of cation-solvating molecules.[27] Such bands, analogously to the most intense DMSO bands, cannot be subtracted from the spectrum of the solution, because they are absent in the spectrum of the pure solvent.[28] Therefore, we determined the IR spectra of different concentrations of Cs_2BCSQ in DMSO solution by subtracting from the spectra of the solution the spectra of an equimolal CsI solution. The latter turned out to be negligibly different from that of pure DMSO. Further, we found that the IR spectra of the cesium, thallium, and sodium salts are different in the solid state, but those of the first two are substantially equal in DMSO solution. The marginal influence of concentration and of the nature of the cation (the ionic radius (Å) with coordination number 6 in crystals is 1.67 for Cs^+, 1.50 for Tl^+, and 1.02 for Na^+)[29] induced us to conclude that the observed solution spectra are due to the little perturbed anion. Unfortunately, such spectra are characterized by extreme differences in the absorbance of the observed bands, which makes it easy to observe only a few strong bands; see Table 3. This drawback was addressed by using concentrated solutions of the very soluble thallium salt. However, DMSO is characterized by strong absorptions, obscuring neighboring $BCSQ^{2-}$ bands. Thus, we also used as solvent DDMSO, but some regions remain covered, and it was necessary to measure the spectra of powdered $BCSQ^{2-}$ salts in the form of mulls to reduce the scattering. In these spectra the absorptions of the mulling agent can be subtracted precisely, because it does not dissolve the salt.

However, the experimental $BCSQ^{2-}$ geometry refers to the $Na_2BCSQ{\cdot}4H_2O$ crystal, and we thought it convenient to obtain the spectrum of this hydrate to check the amount of change of frequencies (or energy) due to the presence of water by comparison with the anhydrous salt. In some regions the absorptions due to water and $BCSQ^{2-}$ may be superposed; the comparison with the deuterated analogue $Na_2BCSQ{\cdot}4D_2O$ provided a clean way to assess the water absorbances.

Inspection of Table 3 shows that the solution and powder spectra are markedly different only in the region of stretching vibrations involving the C≡N, C═O, and C−C(ring) bonds, in agreement with the information provided by the crystal packing. The latter indicates that the dianions form separate entities, whose nitrogens are coordinated, hence interacting, with the cations, oxygen atoms of water, and nitrogen atoms of other dianions, while the oxygens make strong hydrogen bonds with water.

The Raman spectra are less problematic. As apparent from Table 3, several bands of the solution spectrum have intensities that are not very different from the strongest one. Powder spectra are again required to find possible bands in the regions of strong DMSO features. However, all bands remain narrow and with frequency similar to those of the solution spectrum since the mean polarizability is less sensitive than the dipole moment to the molecular environment.[30]

We must also know with these colored samples whether we have coincidence or near coincidence of the exciting 1.064 μm line with an excited-state manifold, which could give a resonance Raman spectrum.[31] The vis−UV−near-IR spectrum of Cs_2BCSQ in DMSO, Figure 2, showed that this is not the case. To reveal possible perturbations of DMSO polarizability produced by the presence of ions, we measured the spectra of the pure solvent and of a 1.0 *m* solution of CsI, but found no noticeable difference.

*3.b. Activity of the Fundamentals.*The molecular dianion $BCSQ^{2-}$ ($C_{10}N_4O_2^{2-}$) as a free unit has 42 normal internal vibrations; in the connectivity represented in Chart 1, its point symmetry is D_{2h}, and the fundamentals then divide into 8 A_g (R, p, α_{xx}), 3 B_{1g} (R, dp), 3 B_{2g} (R, dp), 7 B_{3g} (R, dp), 2 A_u (INS), 7 B_{1u} (IR, *z*), 7 B_{2u} (IR, *y*), and 5 B_{3u} (IR, *x*) vibrations, where INS, R, and IR mean active in inelastic neutron scattering,[32] Raman, and infrared, respectively. As usual, p means polarized, dp depolarized; *x*, *y*, and *z* are the direction of the electrical dipole transition moments. Mutual exclusion of R and IR activity holds for this centrosymmetric unit.

3.c. Selection of the Fundamentals. IR Active. The criteria to propose a band observed in the IR solution spectra (Table 3) as

one of the expected 19 fundamentals are its frequency and intensity, as intrinsic values and relative to the computed ones.[33] An assessment of the usefulness of the latter came from the few bands—the two C≡N, the C═O/ring, ring, and C-ring stretchings—whose frequency ranges are known sufficiently well. The calculations were carried out in the double harmonic (mechanical and electrical) approximation, which led to frequencies on the average slightly higher than the measured ones.

Raman Active. Analogously, the polarized Raman spectrum of the solution of a $BCSQ^{2-}$ salt should provide the frequencies of the 21 g vibrations, from which it should be possible to separate the 8 polarized a_g vibrations. The usefulness of the Raman spectrum is enhanced by the very low intensity calculated and observed for most of the IR-active vibrations.

Proposed Assignment. With reference to Table 5, we now shortly comment on each of the measured spectra, considered in the order which allows buildup of mutually supporting evidences, allowing maximum information to be extracted.

Polarized Raman Spectrum of Na_2BCSQ in DMSO. It appears as a regular spectrum, and allows seven polarized bands to be located, each of which was paired to the a_g vibration nearest in frequency. The eighth was taken as the medium-intensity band at 675 cm^{-1} in the powder spectrum, because the region indicated by the calculations is obscured by DMSO. The overall agreement with the computed values is quite good, and supports the pairing of the depolarized bands to the calculated frequencies on the basis of the frequency value and intensity. As often happens, the g counterparts of very weak u modes give bands of reasonable intensity. A warning as to the quantitative aspect of the calculated intensities comes from the higher intensity of the observed a_g CN stretch (in the unpolarized spectrum) with respect to the b_{3g} stretch, the opposite of what was computed.

Raman Spectrum of Cs_2BCSQ Powder. It appears as a regular spectrum and allows the spectrum in the regions of DMSO bands to be analyzed: 300−400, 600−750, 900−1100, and 1300−1500 cm^{-1}.

IR Spectra of Cs_2DCSQ and Tl_2DCSQ in DMSO Solution and as Mulls. The spectrum of the former substance is characterized by four bands of intensity extraordinarily larger than the others, as expected from the calculations. A saturated solution allows most of the other bands to be localized, whose positions and intensities are supported by the little different spectrum of the more soluble thallium salt. Modes 30 and 1 in Table 5 are calculated in regions obscured by DMSO. The former was associated with the band at 1067 cm^{-1} rather than with that at 966 cm^{-1} of the same intensity in the cesium salt mull owing to the smaller difference with the calculated value. The latter is tentatively paired with the band at 57 cm^{-1} in the cesium mull, which might also be a lattice band. Unassigned remains mode number 18, consistently calculated at about 480 cm^{-1}, because the band at 520 cm^{-1} in the spectrum of the cesium salt mull has no correspondence in the thallium analogue.

IR Spectra of Na_2DCSQ, $Na_2DCSQ{\cdot}4H_2O$, and $Na_2DCSQ{\cdot}4D_2O$ Mulls. In the present context their main function is to support the nature of fundamentals of the bands chosen as such because they are similar in frequency and intensity in all the examined salts. The spectrum of the anhydrous salt shows bands substantially broader than those of the Cs, Tl, and hydrated salts, reflecting the stronger interactions due to the smaller size of the cation and absence of water. The absorbances attributed to H_2O (D_2O) are found at 3550 sh (shoulder), 3515, 3430, 3390, 3270 (2615, 2597, 2522, 2497); 1670, 1655 sh (1223, 1210 sh); and as the very broad feature at 470 (390) cm^{-1}.

Acknowledgment. We thank Professors V. G. Albano for his interest in this work and useful discussions and G. Fini for help with the thermal measurements. Financial support came from the University of Bologna through "Fondi ex-60% and "Funds for selected research topics"; and from MURST Cofin 98.

Supporting Information Available: Tables of crystal data, atomic coordinates, bond lengths and angles, and thermal parameters as well as the CIF file for $Na_2CDCB{\cdot}4H_2O$. This material is available free of charge via the Internet at http://pubs.acs.org.

References and Notes

(1) Busetti, V.; Lunelli, B. *J. Phys. Chem*. **1986**, *90*, 2052.
(2) Mills, I.; Cvitas, T.; Homann, K.; Kallay, N.; Kuchitsu, K. *Quantities, Units and Symbols in Physical Chemistry*, 2nd ed.; Blackwell: Oxford 1993; p 41.
(3) See, for example: Law, K.-Y. *J. Phys. Chem.* **1995,** *99*, 9818 and references therein; *Dyes Pigm.* **1993**, *21*, 1.
(4) Gerecht, B.; Kämpchen, T.; Köhler, K.; Massa, W.; Offermann, G.; Schmidt, R. E.; Seitz, G.; Sutrisno, R. *Chem. Ber*. **1984,** *117*, 2714.
(5) Farnia, G.; Lunelli, B.; Marcuzzi, F.; Sandonà, G. *J. Electroanal. Chem*. **1996**, *404*, 261.
(6) Höhne, G. W. H.; Hemminger, W.; Flammersheim, H.-J. *Differential Scanning Calorimetry*; Springer: Berlin, 1995; (a) p 72, (b) p 110.
(7) Lunelli, B.; Soave, R.; Destro, R. *PCCP* **1999**, *1*, 1469.
(8) North, A. C. T.; Philips, D. C.; Mathews, F. S. *Acta Crystallogr., Sect. A* **1968**, *24*, 351.
(9) Sheldrick, G. M. *SHELXS 86, Program for Crystal Structure Determination*; University of Göttingen: Göttingen, Germany, 1993.
(10) Sheldrick, G. M. *SHELXL 93, Program for Crystal Structure Refinement*; University of Göttingen: Göttingen, Germany, 1993.
(11) Lunelli, B.; Comelli, F. *Rev. Sci. Instrum*. **1987**, *58*, 305.
(12) Rodger, P. M. *Mol. Phys.* **1996**, *89*, 1157. Menger, F. M.; Sanchez, A. M. *Chem. Commun.* **1997**, 199.
(13) Forel, M. T.; Tranquille, M. *Spectrochim. Acta, Part A* **1970**, *26*, 1023.
(14) Hendra, P.; Jones, C.; Warnes, G. *Fourier Transform Raman Spectroscopy*; Ellis Horwood: New York, 1991; p 173.
(15) Parr, R. G.; Yang, W. *Density-Functional Theory of Atoms and Molecules*; Oxford University Press: New York, 1989.
(16) Frisch, M. J.; Trucks, G. W.; Schlegel, H. B.; Scuseria, G. E., Robb, M. A.; Cheeseman, J. R.; Zakrzewski, V. G.; Montgomery, J. A., Jr.; Stratmann, R. E.; Burant, J. C.; Dapprich, S.; Millam, J. M.; Daniels, A. D.; Kudin, K. N.; Strain, M. C.; Farkas, O.; Tomasi, J.; Barone, V.; Cossi, M.; Cammi, R.; Mennucci, B.; Pomelli, C.; Adamo, C.; Clifford, S.; Ochterski, J.; Petersson, G. A.; Ayala, P. Y.; Cui, Q.; Morokuma, K.; Malick, D. K.; Rabuck, A. D.; Raghavachari, K.; Foresman, J. B.; Cioslowski, J.; Ortiz, J. V.; Stefanov, B. B.; Liu, G.; Liashenko, A.; Piskorz, P.; Komaromi, I.; Gomperts, R.; Martin, R. L.; Fox, D. J.; Keith, T.; Al-Laham, M. A.; Peng, C. Y.; Nanayakkara, A.; Gonzalez, C.; Challacombe, M.; Gill, P. M. W.; Johnson, B.; Chen, W.; Wong, M. W.; Andres, J. L.; Gonzalez, C.; Head-Gordon, M.; Replogle, E. S.; Pople, J. A. *Gaussian 98*, Revision A.6; Gaussian, Inc.: Pittsburgh, PA, 1998.
(17) Hariharan, P. C.; Pople, J. A. *Theor. Chim. Acta* **1973,** *28,* 213. Hariharan, P. C.; Pople, J. A. *Chem. Phys. Lett.* **1972,** *66*, 217. Michalska, D.; Bienko, D. C.; Abkowicz-Bienko, A. J.; Lataika, Z. *J. Phys. Chem.* **1996**, *100*, 17786. Czarnik-Matusewicz, B.; Chandra, A. K.; Nguyen, M. T.; Zeegers-Huyskens, T. *J. Mol. Spectrosc.* **1999,** *195*, 308.
(18) El-Azhari, A. A.; Hilal, R. H. *Spectrochim. Acta, Part A* **1997**, *53*, 1365 and references therein.
(19) Handy, N. C.; Murray, C. W.; Amos, R. D. *J. Phys. Chem*. **1993**, *98*, 5612.
(20) Johnson, B. G.; Gill, P. M. W.; Pople, J. A. *J. Chem. Phys*. **1993**, *98*, 5612.
(21) Raghavachari, K.; Trucks, G. W.; Pople, J. A.; Replogle, E. *Chem. Phys. Lett.* **1989**, *158*, 207.
(22) Becke, A. D. *Phys. Rev*. **1988**, *A38*, 3098. Lee, C.; Yang, W.; Parr, R. G. *Phys. Rev*. **1988**, *B41*, 785.
(23) Becke, A. D. *J. Chem. Phys.* **1993**, *98*, 5648.
(24) Whitesides, G. M.; Ismagilov, R. F. *Science* **1999**, *284*, 89 and references therein.
(25) Martinez, J. M.; Pappalardo, R. R.; Marcos, E. S. *J. Chem. Phys.* **1999**, *110*, 1669. Marcus, Y. *Chem. Rev*. **1988**, *88*, 1475.
(26) Kloss, A. A.; Fawcett, W. R. *J. Phys. Chem. A* **1998**, *94*, 1587.
(27) Petersen, C. P.; Gordon, M. S. *J. Phys. Chem. A* **1999**, *103*, 4162.
(28) Loring, J. S.; Fawcett, W. R. *J. Phys. Chem. A* **1999**, *103*, 3608. Leberman, R.; Soper, A. K. *Nature* **1995**, *378*, 364.

(29) Lide, D. R., Ed. *Handbook of Chemistry and Physics*, 78th ed.; CRC Press: Boca Raton, FL, 1998; Chapter 12, p 14.
(30) Hollas, J. M. *High-Resolution Spectroscopy*; Butterworths: London, 1982; p 153.
(31) Strommen, D. P. *J. Chem. Educ.* **1992**, *69*, 803.
(32) Eckert, J. *Spectrochim. Acta, Part A* **1992**, *48*, 271.
(33) Kjaergaard, H. G.; Bezar, K. J.; Brooking, K. A. *Mol. Phys.* **1999**, *96*, 1125.